

Stimulus Response Detection in fMRI Using Temporal Clustering Analysis, Digital Filters and a Two-Dimensional Neighbourhood Test

Sarah Lee^{1,2,*}, Fernando Zelaya³, Stephanie A. Amiel² and Michael J. Brammer¹

¹Brain Image Analysis Unit,
Institute of Psychiatry,
King's College London,
London. SE5 8AF
United Kingdom

²Diabetes Research Group,
School of Medicine at
King's College Hospital,
King's College London,
London. SE5 9PJ United Kingdom

³Institute of Psychiatry,
King's College London,
London. SE5 8AF
United Kingdom

{*sarah.lee@iop.kcl.ac.uk}

*Tel: +44-20-7919-3045

ABSTRACT

A model-free fMRI (functional magnetic resonance imaging) analysis method is proposed to detect gradually evolving physiological or pharmacological responses to a single-event or non-repetitive multi-event experiment without any a priori information on the paradigm. The method is developed from the pre-existing temporal clustering analysis method with the applications of digital filters, temporal averaging and a two-dimensional constraint test and makes use of the data from the whole brain instead of a selected single slice. We have applied the technique to the fMRI data from two different kinds of experiments and the results demonstrate that our method is able to identify brain regions and time bins during which the BOLD (blood oxygenation level dependent) MRI time series display responses to sensory stimuli.

1: INTRODUCTION

fMRI is one of the techniques most widely used to study brain activity and cognition. The analysis of fMRI data allows us to understand how the brain responds to specific stimuli. Analysis methods can be broadly divided into two categories: model-based and model-free methods. For the model-based methods the detection of brain activation is carried out by comparing the temporal series of images to a model, which is based on the expected temporal variation of the signal intensity [3]. In contrast, model-free techniques do not employ such a model [3]. Instead, signal processing tools are used to extract the main components of the signal variance.

Recently, a series of temporal clustering analysis (TCA) methods have been proposed as an alternative tool of model-free techniques. These include original TCA [6], modified TCA (MTCA) [10], and iterative TCA [4]. All these methods are based on processing the temporal information of a single fMRI slice ($Y \times X \times T$, where Y and X are the number of voxels in y and x axes respectively of each fMRI image and T is the number of volumes acquired during the experiment). The data are

transformed to a two-dimensional representation, in which the total number of voxels that reach a maximum at each time point are computed for every point of the time series. In TCA with a 2D neighbourhood test [5], the spatial information available within a slice is also used to take advantage of the observation that physiologically plausible brain activations seldom occur in single isolated voxels.

The work presented here is an extension of the TCA approach [5] incorporating an additional moving-average filter to improve the elimination of high-frequency noise in the data. In addition, we have optimised the design of a bandpass filter, in order to remove low frequency noise and restrict the search to the temporal width of the responses expected in our chosen paradigm. Furthermore, we use a 2D neighbourhood test to eliminate spurious false positive sometimes found in small clusters and stand alone voxels, which do not belong to any cluster. The number of voxels detected in all available slices is also taken into account in stimulus response detection instead of just the voxels within a single slice.

2: METHOD

2.1: Initial data processing

Firstly, the fMRI time series ($Y \times X \times T \times S$, where $Y \times X$ are the number of voxels in y and x axes respectively for each image plane, T is the number of volumes and S is the number of slices acquired during the experiment) is motion corrected using XBAM [1] and a brain mask is obtained employing the FSL brain extraction tool [9]. The method takes a slice of data at one time [2], in matrix form: $\underline{D}_{ori,s}$ of size $Y \times X \times T$, where s denotes the s -th slice on transverse section. The M valid voxels obtained from the mask of slice s corresponding to the brain tissue are distributed at co-ordinates $\left[\underline{m}_{(s,y)}; \underline{m}_{(s,x)} \right]$, where

$$\underline{m}_{(s,y)} = \left[m_{(s,y_1)}, m_{(s,y_2)}, \dots, m_{(s,y_M)} \right]$$

$\underline{m}_{(s,x)} = [m_{(s,x_1)}, m_{(s,x_2)}, \dots, m_{(s,x_M)}]$, and $(m_{(s,y_i)}, m_{(s,x_i)})$ are the y and x co-ordinates respectively of the i -th voxel corresponding to the brain tissue in the slice S . Thus, the time series of voxels representing brain tissue in slice S are $\underline{D}_{ori,s}(m_{(s,y_\mu)}, m_{(s,x_\mu)}, \tau)$, where $\mu = 1, \dots, M$ and $\tau = 1, \dots, T$. This 3-D information is reduced to two dimensions in the MTCA methods as $\underline{D}_{2D,s}$ [4, 6, 10], a $M \times T$ matrix in Appendix (1) and as in [5] we work in the percentage of signal change (psc) instead of the actual intensity. The percentage of signal change for each time series is calculated using $\underline{D}_{psc,s} = (\underline{D}_{2D,s} - \underline{D}_{exp,s}) ./ \underline{D}_{exp,s} \times 100\%$, where $./$ indicates the element-by-element division for two matrices,

$$\underline{D}_{exp,s} = \begin{bmatrix} E\{\underline{D}_{2D,s}(1,:)\} & \dots & E\{\underline{D}_{2D,s}(1,:)\} \\ \vdots & \ddots & \vdots \\ E\{\underline{D}_{2D,s}(M,:)\} & \dots & E\{\underline{D}_{2D,s}(M,:)\} \end{bmatrix}, \quad \text{a } M \times T$$

matrix and $E\{\cdot\}$ denotes the expectation operation.

2.2: Moving Average and Bandpass Filtering Processes

At this stage, a moving average is applied to each time series, i.e., each row of $\underline{D}_{psc,s}$. The bandpass filter is also applied here, in order to eliminate low and high frequency artefact. Details of the bandpass filter designed for this work can be found in Section 4. The matrix containing filtered time series is denoted as $\underline{D}_{filtered,s}$ of size $M \times T$.

2.3: Temporal Averaging

As in [5], the data are now grouped in time bins, i.e., the average of every non-overlapping n time points in $\underline{D}_{filtered,s}$. The matrix that proceeds to the next stage is $\underline{D}_{analysis,s}$, a $M \times (T/n)$ matrix in Appendix (2).

2.4: Locating Maximum Response

For each voxel time series the time bin of observed maximum is found. The binary matrix $\underline{R}_{max,s}$ of size $M \times (T/n)$ reflects the maximum signal for each voxel in $\underline{D}_{analysis,s}$ and is formed as Appendix (3). Another binary matrix, $\underline{D}_{checking,s,\tau}$, of size $Y \times X$ is generated for obtaining the spatial distribution information of voxels which reach their maxima at time bin τ :

$$\underline{D}_{checking,s,\tau}(m_{(s,y_\mu)}, m_{(s,x_\mu)}) = \begin{cases} 1, & \text{if } \underline{R}_{max,s}(\tau, \mu) = 1 \\ 0, & \text{otherwise} \end{cases} \quad (4)$$

for $\tau = 1, \dots, T/n$ and $\mu = 1, \dots, M$.

In the conventional TCA methods [4, 6, 10], the matrix $\underline{R}_{max,s}$ is summed column wise, so that the time window with the maximum number of voxels reach their

maxima may be identified using equation (5) for each point in the time series.

$$\underline{F} = [F_1, F_2, \dots, F_{T/n}] \quad \text{where } F_k = \sum_{j=1}^M \underline{R}_{max,s}(j, k) \quad (5)$$

In our method, before this summation takes place, for every time bin a two-dimensional neighbourhood test is applied to all voxels which are detected to have reached their maxima.

2.5: Two-Dimensional Neighbourhood Test

A 2-D neighbourhood test [5] is applied at this stage to include only clusters of connected voxels. We use an improved method to define the minimum threshold to determine the number of connected voxels.

In $\underline{D}_{checking,s,\tau}$, a 3×3 neighbourhood is formed for each maximum. For example, if a voxel reaches its maximum at time τ is at co-ordinate $(m_{(s,y_\alpha)}, m_{(s,x_\alpha)})$, its number of neighbours in a 3×3 neighbourhood which also reach a maximum is $N_{s,\tau}[m_{(s,y_\alpha)}, m_{(s,x_\alpha)}]$ in equation (6).

$$N_{s,\tau}[m_{(s,y_\alpha)}, m_{(s,x_\alpha)}] = \left[\sum_{y'=m_{(s,y_\alpha)}-1}^{m_{(s,y_\alpha)}+1} \sum_{x'=m_{(s,x_\alpha)}-1}^{m_{(s,x_\alpha)}+1} \underline{D}_{checking,s,\tau}(y', x') \right] - 1 \quad (6)$$

The number of neighbouring voxels that each maximum voxel has is recorded and only the voxels with the number of neighbouring voxels in the upper 20% of the frequency versus number of neighbours histogram, are taken into account. This number of neighbouring voxels threshold is denoted as γ .

A new matrix, $\underline{R}'_{max,s}$, is formed to count the number of voxels that have passed the 2D neighbourhood test.

$$\underline{R}'_{max,s}(\mu, \tau) = \begin{cases} 1, & \text{if } N_{s,\tau}[m_{(s,y_\mu)}, m_{(s,x_\mu)}] \geq \gamma \\ 0, & \text{otherwise} \end{cases} \quad (7)$$

for $1 \leq \mu \leq M$ and $1 \leq \tau \leq T/n$.

The matrix $\underline{R}'_{max,s}$ is then summed column wise to identify the time bin when the maximum number of voxels, which meet our selection criteria, reach their maxima.

$$\underline{F}'_s = [F'_1, F'_2, \dots, F'_{T/n}], \quad \text{where } F'_q = \sum_{p=1}^M \underline{R}'_{max,s}(p, q) \quad (8)$$

2.6: Stimulus Detection

For all the available S slices, $\underline{F}' = \sum_{s=0}^{S-1} \underline{F}'_s$, a $1 \times T/n$ vector, returns the number of voxels that reach a maximum and meet our selection criteria at each time bin. For an experiment involving κ stimuli, we record the first 2^κ time bins with the largest number of maximum

voxels which survive the test (they are referred to as first maximum, second maximum, so on) and generate their corresponding activation maps.

3: EXPERIMENTS

The proposed method was applied to five sets of fMRI data from two different experiments.

Experiment 1: Visual Stimulus

A 8-Hz flickering checkerboard visual stimulus was presented to a healthy subject between 60-120 seconds during an experiment lasting 300 seconds with repetition time (TR) = 2 seconds. 150 volumes of 20 transverse slices were acquired with voxel dimensions: 3.75mm × 3.75mm × 5.5mm. Four sets of data were acquired for method validation: VIS1, VIS2, VIS3 and VIS4.

Experiment 2: Visual and Auditory Stimuli

Two types of stimuli were involved: visual and auditory. The visual stimulus was presented between 60-120 seconds and the auditory stimulus between 210-274 seconds. The experiment, again, lasted 300 seconds and 150 volumes of 25 transverse slices with TR=2 seconds were acquired. Voxel dimensions: 3.75mm × 3.75mm × 5.5mm. One data set was acquired: VIS-AUD.

4: PARAMETERS USED IN THE APPLICATION TO fMRI DATA

A 5-point moving average filter is used for all experiments. For the digital Butterworth bandpass filter, the normalised passband frequency range is $[40/T, 80/T]$ and the normalised stopband frequencies are at $20/T$ and $100/T$ for all experiments. The filters are implemented in Matlab [7, 8]. The parameter n for the temporal averaging is 5, which result in every time bin equal to 10 seconds. The γ for the 2D neighbourhood test can be found in Table 1 with details of the occurrences of all number of neighbouring voxels (0 to 8) in the 3×3 neighbourhood for all voxels.

5: RESULTS

The temporal and spatial information obtained after applying our method for all five sets of data can be found in Table 2. For VIS1-4, where there was only one stimulus, the time bins associated with first and second maximum number of voxels reaching their maxima were identified. For the VIS-AUD, the time bins corresponding to clusters containing the four largest number of voxels were found, since there were two stimuli. The activation maps are given for the results having a superscript in Table 2, which indicates the Fig. number. Due to the space constraints, only three slices are displayed for each case.

6: DISCUSSION

The results in Table 2 show that our method is able to detect the time bins, during which the brain activation was expected to the sensory stimulus in VIS1-3 and VIS-AUD. In both VIS1 and VIS2, the time bin associated with the maximum number of voxels that met our selection criteria fell in 70-80 seconds and 80-90 seconds, which were right after the visual stimulus was on. Their activation maps in Fig. 1 and 2 show activation in primary visual and extrastriate visual areas. In VIS3, the second maximum happened during the time bin 70-80 seconds and the activation map in Fig. 3 clearly shows that the primary and extrastriate visual areas contributed to this maximum.

For VIS4, the time bins detected did not fall into the period when the visual stimulus was on. In order to investigate it further, the time series were extracted from both this data set and VIS1 for comparison. The average time series for each slice shown in Fig. 1 are given in Fig. 6-8 respectively for VIS1, in which the time series in percentage of change were plotted in blue with the filtered and temporally averaged data in dots. They clearly show a peak ongoing for about 30 seconds starting from the 70th seconds. For VIS4, the first maximum was detected during the time bin 220-230 seconds. Three slices are shown here in Fig. 9 and their average time series are displayed in Fig. 10-12 respectively. The percentages of change showed a peak with the characteristics that fell into our selection criteria, hence this time bin was detected. In order to understand why the visual stimulus was not detected in this case, time series in the visual areas were extracted to examine whether the peak has been missed by our method or not. The time series from primary visual and extrastriate visual areas were extracted from Slice 8 and 9 and their averages can be found in Fig. 13-16 with the chosen voxels; no peak with our desired temporal width was found in them.

For the data set that involved two stimuli, VIS-AUD, we examined the four time bins associated with the first four maximum number of voxels that met our selection criteria. In the third and fourth maxima, the time bins fell into the period when the auditory and visual stimuli were on respectively. Fig. 4 shows activation in auditory association cortex and the activations in primary and extrastriate visual areas can be found in Fig. 5.

7: CONCLUSION

A model-free fMRI analysis method for single-event and non-repetitive multiple event experiments is proposed employing the conventional temporal clustering analysis technique with additional digital filtering processes and a two-dimensional neighbourhood test and all available slices are taken into account. The results from the application to two types of experiments involving single visual stimulus and both visual and auditory stimuli demonstrate that our method is able to detect the peaks in order of 1.5-2% which are typically found in the fMRI experiment in time series that meet our selection criteria and 80% of the time these peaks correspond to the stimulus spatially and temporally.

7: ACNOWLEDGEMENT

The authors would like to thank Wellcome Trust for the project funding.

REFERENCES

- [1] E.T. Bullmore, M.J. Brammer, S. Rabe-Hesketh, V. Curtis, R.G. Morris, S.C.R. Williams, T. Sharma and P.K. McGuire, "Methods for diagnosis and treatment of stimulus-correlated motion in generic brain activation studies using fMRI", *Human Brain Mapping*, Vol. 7, pp. 38-48, 1999.
- [2] EEG/MRI Matlab Toolbox, <http://eeg.sourceforge.net>.
- [3] Jezzard, P.M. Matthews and S.M. Smith (editors), *Functional MRI an introduction to methods*, Oxford University Press, 2001.
- [4] J.-H. Gao, and S.-H. Yee, "Iterative temporal clustering analysis for the detection of multiple response peaks in fMRI", *Magnetic Resonance Imaging*, Vol. 21, pp. 51-53, 2003.
- [5] S. Lee, F. Zelaya, L. Reed, M.J. Brammer and S.A. Amiel, "A model-free method for fMRI analysis using temporal clustering and neighbourhood constraint", *12th Annual Meeting of the Organization for Human Brain Mapping*, 2006.
- [6] Y. Liu, J.-H. Gao, H.-L. Liu and P.T. Fox, "The temporal response of the brain after eating revealed by functional MRI", *Nature*, Vol. 405, pp. 1058-1062, 2000.
- [7] Matlab, Signal Processing Toolbox, The Mathworks, Inc.
- [8] S.K. Mitra, *Digital Signal Processing a computer-based approach*, McGraw-Hill International Editions, Electrical Engineering Series, 1998.
- [9] S.M. Smith, "Fast robust automated brain extraction", *Human Brain Mapping*, Vol. 17, No. 3, pp. 143-155, 2002.
- [10] S.-H. Yee and J.-H. Gao, "Improved detection of time windows of brain responses in fMRI using modified temporal clustering analysis", *Magnetic Resonance Imaging*, Vol. 20, pp. 17-26, 2002.

$N_{0:S-1;T/n}$	VIS1	VIS2	VIS3	VIS4	VIS-AUD
0	4087	4971	4150	4487	3909
1	3330	4122	3640	3785	3518
2	2502	2999	2809	2789	2694
3	1788	2226	2356	2084	2054
4	1188	1534	1600	1456	1508
5	707	1124	1133	914	993
6	376	674	642	465	692
7	171	370	387	235	465
8	50	164	222	87	316
Total	14199	18184	16939	16302	16149
γ	4	5	5	4	5

Table 1. The frequency of the number of neighbouring voxels each maximum voxel has and the γ threshold for the 2D neighbourhood test for all the fMRI data sets.

Data	First Max	Second Max	Third Max	Fourth Max
VIS1	V 70-80 ¹	200-210	-	-
VIS2	V 80-90 ²	280-290	-	-
VIS3	230-240	V 70-80 ³	-	-
VIS4	220-230 ⁹	260-270	-	-
VIS-AUD	0-10	280-290	A 220-230 ⁴	V 70-80 ⁵

Table 2. The temporal (time bin) and spatial information obtained for give sets of fMRI data using the proposed method. A and V indicate the responses corresponding to auditory and visual stimuli respectively. The superscript number indicates the figure number for the activation map.

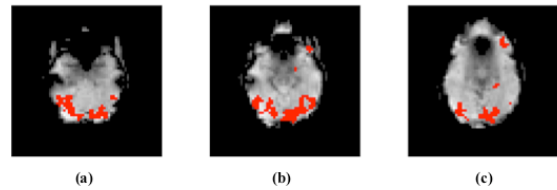


Fig. 1. Experiment: VIS1. The activation map of the first maximum detected at time bin: 70-80 seconds.

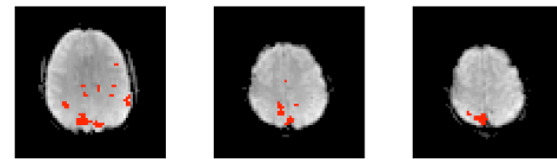


Fig. 2. Experiment: VIS2. The activation map of the first maximum detected at time bin: 80-90 seconds.

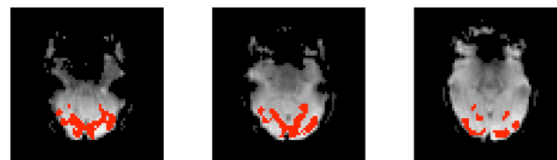


Fig. 3. Experiment: VIS3. The activation map of the second maximum detected at time bin: 70-80 seconds.

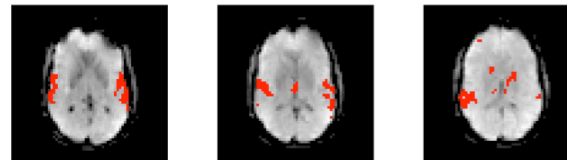


Fig. 4. Experiment: VIS-AUD. The activation map of the third maximum detected at time bin: 220-230 seconds.

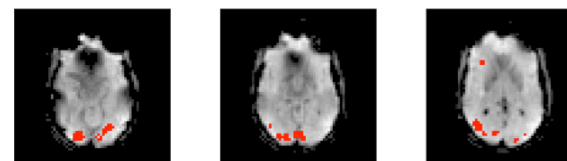


Fig. 5. Experiment: VIS-AUD. The activation map of the fourth maximum detected at time bin: 70-80 seconds.

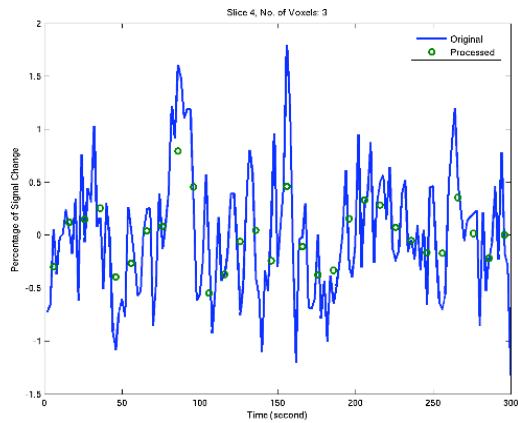


Fig. 6. The average original and processed time series for activated voxels found in Fig. 1(a).

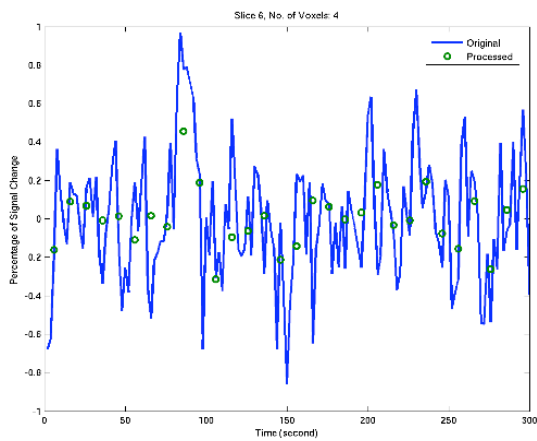


Fig. 7. The average and processed time series for activated voxels found in Fig 1(b).

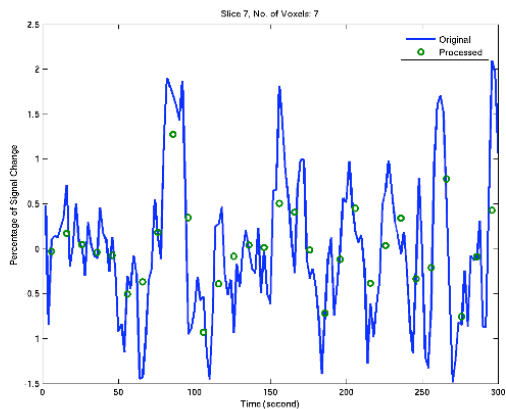


Fig. 8. The average original and processed time series for activated voxels found in Fig. 1(c).

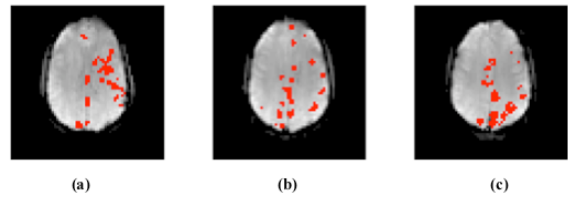


Fig. 9. Experiment: VIS4. The activation map for the first maximum detected at time bin: 220-230 seconds.

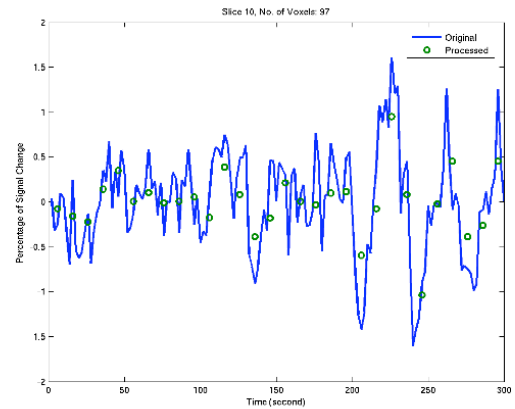


Fig. 10. The average original and processed time series for activated voxels found in Figure 9(a).

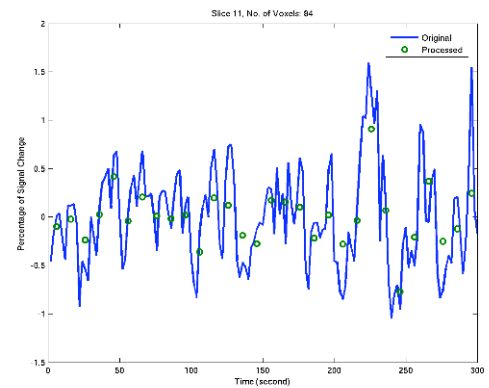


Fig. 11. The average original and processed time series for activated voxels found in Fig. 9(b).

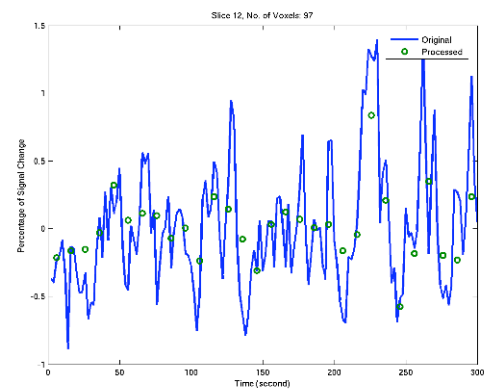


Fig. 12. The average original and processed time series for activated vowels found in Fig. 9(c).

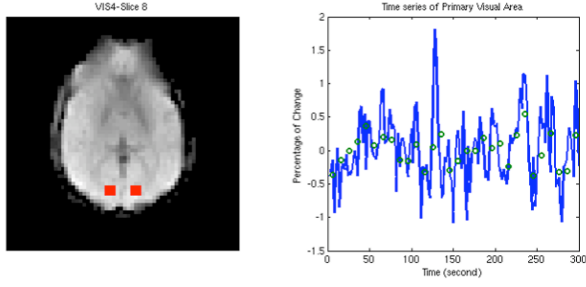


Fig. 13. The average original and processed time series for VIS4 in the primary visual area: Slice 8.

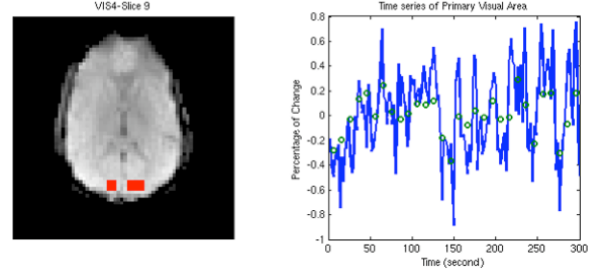


Fig. 15. The average original and processed time series for VIS4 in the primary visual area: Slice 9.

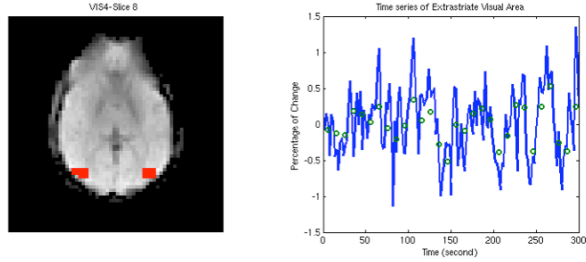


Fig. 14. The average original and processed time series for VIS4 in the extrastriate visual area: Slice 8.

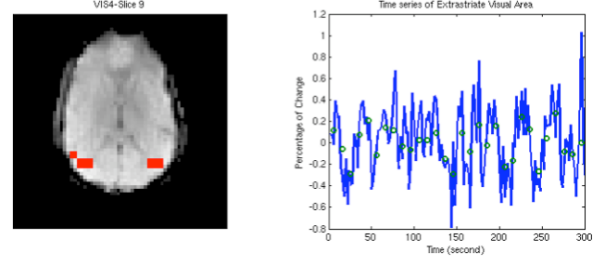


Fig. 16. The average original and processed time series for VIS4 in the extrastriate visual area: Slice 9.

APPENDIX

$$\underline{\mathbf{D}}_{2D,s} = \begin{bmatrix} \underline{\mathbf{D}}_{ori,s}(m_{(s,y_1)}, m_{(s,x_1)}, 1) & \underline{\mathbf{D}}_{ori,s}(m_{(s,y_1)}, m_{(s,x_1)}, 2) & \cdots & \underline{\mathbf{D}}_{ori,s}(m_{(s,y_1)}, m_{(s,x_1)}, T) \\ \underline{\mathbf{D}}_{ori,s}(m_{(s,y_2)}, m_{(s,x_2)}, 1) & \underline{\mathbf{D}}_{ori,s}(m_{(s,y_2)}, m_{(s,x_2)}, 2) & \cdots & \underline{\mathbf{D}}_{ori,s}(m_{(s,y_2)}, m_{(s,x_2)}, T) \\ \vdots & \vdots & \ddots & \vdots \\ \underline{\mathbf{D}}_{ori,s}(m_{(s,y_M)}, m_{(s,x_M)}, 1) & \underline{\mathbf{D}}_{ori,s}(m_{(s,y_M)}, m_{(s,x_M)}, 2) & \cdots & \underline{\mathbf{D}}_{ori,s}(m_{(s,y_M)}, m_{(s,x_M)}, T) \end{bmatrix} \quad (1)$$

$$\underline{\mathbf{D}}_{analysis,s} = \begin{bmatrix} E\{\underline{\mathbf{D}}_{filtered,s}(1, 1:n)\} & E\{\underline{\mathbf{D}}_{filtered,s}(1, n+1:2n)\} & \cdots & E\{\underline{\mathbf{D}}_{filtered,s}(1, T-n+1:T)\} \\ E\{\underline{\mathbf{D}}_{filtered,s}(2, 1:n)\} & E\{\underline{\mathbf{D}}_{filtered,s}(2, n+1:2n)\} & \cdots & E\{\underline{\mathbf{D}}_{filtered,s}(2, T-n+1:T)\} \\ \vdots & \vdots & \ddots & \vdots \\ E\{\underline{\mathbf{D}}_{filtered,s}(M, 1:n)\} & E\{\underline{\mathbf{D}}_{filtered,s}(M, n+1:2n)\} & \cdots & E\{\underline{\mathbf{D}}_{filtered,s}(M, T-n+1:T)\} \end{bmatrix} \quad (2)$$

$$\underline{\mathbf{R}}_{max,s}(\mu, \tau) = \begin{cases} 1, & \text{if } \underline{\mathbf{D}}_{analysis,s}(\mu, \tau) \text{ is } \max\{\underline{\mathbf{D}}_{analysis,s}(\mu, :)\} \\ 0, & \text{otherwise} \end{cases} \quad \text{for } 1 \leq \mu \leq M \text{ and } 1 \leq \tau \leq T/n \quad (3)$$